HALL THRUSTER 3D PLUME MODELING AND COMPARISON WITH SMART-1 FLIGHT DATA

A.Vicini[(1)], A.Passaro,[(2)], L.Biagioni[(1)]

[(1)] Alta S.p.A., via Gherardesca 5, Ospedaletto (PI), 56121, Italy
[(2)] CPR-Aerospace Division, – via Gherardesca5, Ospedaletto (PI), 56121, Italy

ABSTRACT

Electric propulsion represents one of the most promising technologies for application in future space missions; Hall Effect Thrusters (HET's) and Gridded Ion Engines (GIE) are particularly interesting for their relatively high thrust capability coupled with a specific impulse which is up to one order of magnitude higher than latest generation chemical systems.

The knowledge of the plasma plume evolution in the thruster surrounding space is of fundamental importance, at system design level, for new generation satellites, in order to integrate the propulsive subsystem with the other vehicle subsystems: as known, the use of electro-magnetic thrusters can create compatibility problems, due to the electrically charged particle flow, which can interfere with telecommunication signals and generate erosion and insulation loss for critical satellite surfaces (e.g. solar panels, optical instruments and sensors etc.).
A number of Hall thruster plume models have been developed[1]; present simulation techniques usually implement a Particle In Cell / Monte Carlo approach to a plasma flow considered in a quasi-neutral state, with the possibility of a residual atmosphere (typical of a vacuum chamber test facility). In this paper the 3D plume simulation model developed by Alta will be described, and applied to model the SNECMA PPS®1350 thruster used on the SMART-1 satellite.

1. INTRODUCTION

During the last few years numerical activities at Alta S.p.A and CPR, in Pisa, Italy, have been focused on plasma thruster plume simulation and interaction of the plume with spacecraft or vacuum chamber environment: two *hybrid* PIC-MCC codes (one for axysimmetric simulation, one for 3D configurations) and a *neutral* DSMC code have been developed for simulations of realistic vacuum chamber geometries.

Besides the correct physical modelling of the relevant phenomena which takes place in the thruster plasma plume, one of the most delicate point for the thruster plume simulation regards the conditions used to describe the plasma at the exit of the acceleration channel, which are an input for plume simulation code. Among the others, such conditions include ions potential, number density and velocity distributions, and electron temperature. As a matter of fact, only using conditions closely resembling the actual ones may result in a reliable simulation of the plume features. The problem is that a complete characterization of the plasma characteristics in the thruster exit plane is usually not available. Most often accessible experimental results consist of current density measurements on rakes inside the plume; other data such as local RPA measurements may sometimes be available. On the other hand, in the development phase of a new thruster of course no experimental data exist; in this case, numerical models of the thruster can be used to simulate the plasma inside the acceleration channel, and the results obtained used as an input for the subsequent plume simulation. In both cases, not all of the needed data can be derived from experiment or other numerical tools. It is thus generally necessary to use data deriving from similar configurations; these may possibly be subsequently adjusted through an assessment of the results obtained.
After a brief description of the code, the present paper will illustrate the results obtained for the simulation of the PPS®1350 Hall thruster installed on the SMART-1 satellite. Ions injection conditions for this case are first obtained by comparison with an available current density distribution obtained in the vacuum chamber. These conditions are then used to simulate the thruster in flight conditions. The sensitivity of the results to other physical parameters will be described. A comparison with flight data measurements will also be illustrated.

2. CODE DESCRIPTION

The PICPluS3D code, developed at Alta, is a hybrid particle-fluid model. The Particle In Cell (PIC) is employed to model the plasma dynamics, and direct simulation Monte Carlo (MCC or DSMC) is used to simulate the collisions dynamics.

2.1 Plasma Dynamics

The plasma potential is obtained by the hypothesis of quasi-neutrality, and thus equalling the electron density to the ion density. Assuming that electrons are collisionless and un-magnetized, and that their pressure

obeys the ideal gas law, the Boltzmann relation is obtained for the plasma potential:

$$\varphi - \varphi^* = \frac{kT}{e} \ln(\frac{n}{n^*}) \quad (1)$$

where superscript * indicates a reference state. The electric field is obtained through spatial differentiation of the plasma potential. Electron temperature in eq.(1) may be held constant. However, as experimental evidence indicates that electron temperature is not constant, an adiabatic model can be used to relate its changes to changes in electron density:

$$T = T_{ref} \left(\frac{n}{n_{ref}} \right)^{\alpha - 1} \quad (2)$$

where α is a number than can be set between $\gamma = c_p / c_V$ = 5/3 (monoatomic gas) and 1 (isothermal case); in this case the electron temperature field is updated at each time step. A static magnetic field can also be included in the simulation.

2.2 Ions and Neutrals

Several particle species can be independently simulated. Xenon propellant is currently used, but other propellants can be added. Background distributions of neutral propellant are included in the simulation. Neutral atoms, possibly exiting from the thruster due to the effective ionization rate, are also simulated (either through a MCC or DSMC approach[2,3]).

2.3 Collision Dynamics

Neutral-neutral and ion-neutral (elastic and Charge Exchange (CEX)) collisions can be included in the PIC cycle independently. In the case of atom-atom collisions, the Variable Hard Sphere (VHS) model is employed. For atom-ion collisions, the VHS model or the induced dipole model of Nanbu[4] can be used; in the latter case, no collision cross sections need to be modelled.

2.4 Computational Grid

The computational grid is cartesian, non uniform in every direction in order to adapt to the local plasma density in a simple and straightforward way. This allows to model fairly complex geometries, while providing good computational efficiency for particles tracking operations.

2.5 Boundary conditions

The boundaries of the simulation domain can be considered as outflow or as solid walls; in the latter case their temperature and potential are assigned, and ion impacts may range between perfect reflection and full random diffusion, with partial thermal accommodation calculated using Cercignani-Lampis-Lord model[2]. In the same manner internal solid boundaries can be modelled.

Data regarding the plasma characteristics at the exit of the thruster (potential, number densities, velocities) can be customized so as to represent the desired distributions.

3. SMART-1 SIMULATION AND COMPARISON WITH FLIGHT DATA

An application to the simulation of the PPS®1350 thruster installed on the SMART-1 satellite will here be presented. SMART-1 is the first ESA Small Mission for Advanced Research & Technology, conceived to demonstrate the operation and the effectiveness of Solar Electric Propulsion for deep space cruising. The satellite has been launched on September 27th 2003, with the mission of reaching the Moon and orbit it for a period of 6 months. Extensive use of HET is made to spiral out from the initial GTO and reach the Moon's gravitational field. A specific instrument, the Electric Propulsion Diagnostic Package (EPDP), has been developed by LABEN Proel Tecnologie Division (LABEN/Proel)[5] for the monitoring of the operation/environment of the electric propulsion system. The EPDP operates in conjunction with another instrument, named SPEDE (Spacecraft Potential Electron and Dust Experiment); in this way, a comprehensive evaluation of performance and effects of the electric propulsion system based on the PPS®1350 thruster developed by SNECMA can be obtained. While the EPDP provides information on the plasma environment near the thruster, SPEDE characterizes the plasma on the spacecraft sides. The EPDP collects information on the following areas:

- energy/current distribution of plasma ions close to the plasma beam;
- plasma electronic parameters (e.g. plasma density, potential and electron temperature);
- material erosion/deposition at the Quartz Crystal Microbalance location;
- Solar Cell performance (V-I measurement in open, load, short condition).

The nominal characteristics of the thruster used in the simulations are summarized in Table 1.

Table 1 – PPS1350 simulation nominal characteristics.

Propellant flow rate (anode)	4.21 10^{-6} kg/s
Discharge voltage	350 V
Discharge current	3.47 A
Thrust	72.1 mN

An assessment of the plume simulation has been carried out using the corresponding experimental data;

for this case, a current density rake measured at a distance of 0.65 m from the thruster in a vacuum chamber facility was available from SNECMA, together with RPA measurements of the LABEN EPDP device in flight conditions. The experimental current density was used in a preliminary investigation with the purpose to obtain the ions ejection conditions from the thruster that best fit the experimental distribution. To this purpose, the ions distributions at the exit of the acceleration channel are represented using Gaussian distributions for both number density and velocity angle. This investigation was carried out using the axysymmetric version of the PICPluS code[6], with a background pressure $p = 1 \cdot 10^{-2}$ Pa. Fig.1 shows the comparison between the experimental and the computed current density; the results obtained using exit conditions similar to those characteristic of an SPT-100 thruster, which were used as starting guess, are also illustrated. The final "optimum" ions exit conditions are rather different from the starting ones; besides, it is apparent that a probe bias also need to be simulated to fit the experiment. The adiabatic model was used for electron temperature, and 25% of double charged ions were assigned to match the thruster performances (thrust, beam current).

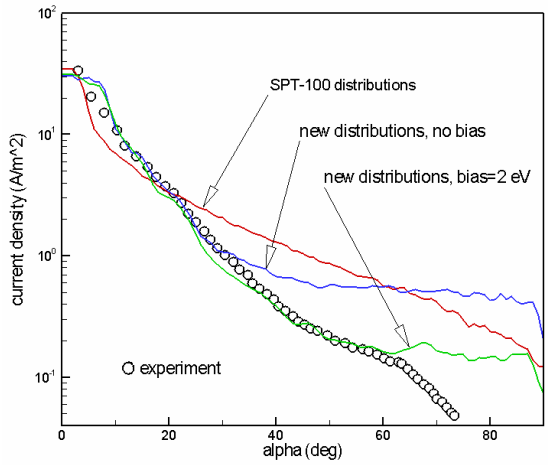

Fig.1 – Experimental and computed current densities for the PPS1350 HET thruster.

These conditions were subsequently used for the 3D plume simulation in flight conditions. The geometry model used for the satellite is illustrated in Fig.2, together with a sketch of the computational grid; it includes the satellite main body and part of the solar cells panels, and the extension of the simulation domain is 2 m in every direction from the thruster. The grid size is 64x64x68 cells, and about $3 \cdot 10^6$ particles (Xe^+ and Xe^{++}) were used for the simulations described in the following.

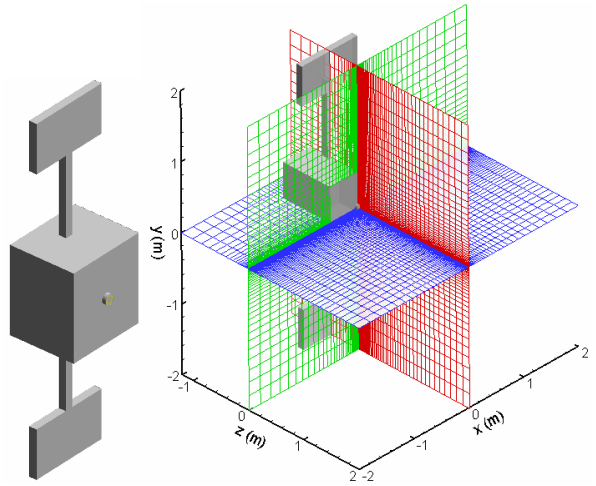

Fig.2 - Sketch of the geometry model and of the computational grid used for the SMART-1 test case.

Fig.3 shows the shape of the computed plume; no appreciable backflow is predicted. The computed current density is shown in Fig. 4, compared with the experimental one and with that obtained through 2D simulations in vacuum chamber conditions. It can be seen that in flight conditions the whole plume shape is changed, also at low angles; the plume is more focused, and this also results in a higher computed thrust (about 10%). As with the 2D simulations, electron temperature was computed using the adiabatic model with α=4/3, and setting a value of approximately 8 eV at the exit of the thruster.

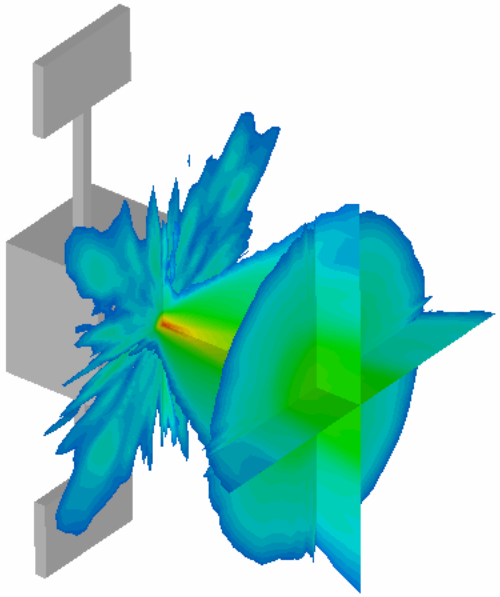

Fig.3 – Shape of the computed plume

The EPDP RPA instrument is located on the same face of the satellite of the thruster, at a distance of 0.47 m from the latter, and of about 0.05 m from the satellite face. Fig.5 shows the comparison between charge

exchange ions energy distributions obtained from the RPA measurements and the corresponding computation obtained using a virtual instrument.

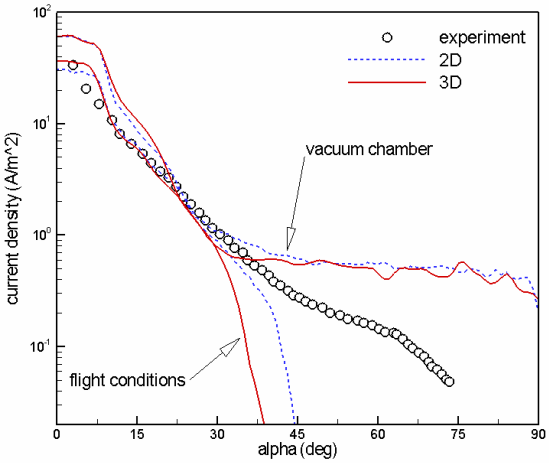

Fig.4 – Comparison of current densities obtained by 2D and 3D simulations.

It can be seen how the energy peak in the measure is found at approximately 36 eV, while in the simulation it is at approximately 18 eV. From the EPDP measurements it can be observed, as illustrated in Fig.6, that the floating potential rises with time, and the energy corresponding to the RPA distribution peak rises in a similar fashion, with a difference of about 18 V between the two values, showing that the actual potential of the distribution peak w.r.t. the RPA instrument is 18V. If the experimental distribution is shifted accordingly, see Fig.5, a quite good agreement is obtained for the primary energy peak, and also the secondary peak, which is due to the presence of double charged ions in the simulation, is well represented.

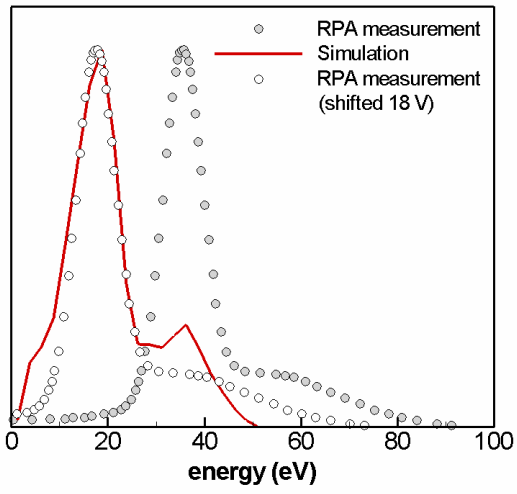

Fig.5 – Measured and simulated plasma energy distribution.

The magnitude of the secondary peak is dependent on the percentage of double charged ions, here arbitrarily set to 25%. The high energy tail shown by the measurement above 50 eV is missing in the computation; this could be possibly obtained by using longer sampling times for the virtual probe, as "events" up to 100 eV are recorded in the simulation. In any case, further investigations on the correct interpretation of the measured energies and comparison with the computed ones need to be carried out.

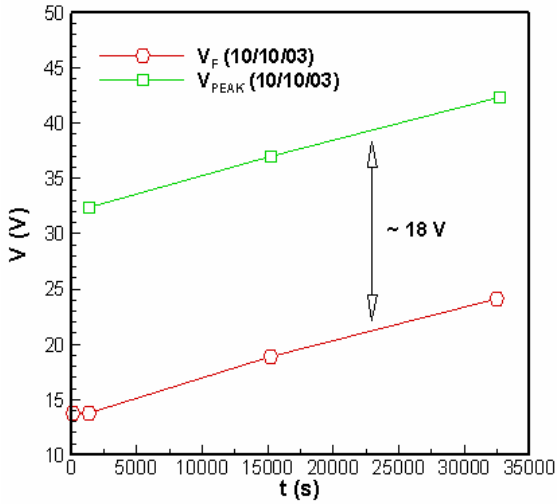

Fig.6 – Measured floating potential and energy of the RPA distribution peak.

In order to assess the sensitivity of the CEX energies to the electron temperature, two other simulations were carried out increasing the reference electron temperature, so as to obtain values of approximately 12 and 16 eV, respectively, at the exit of the acceleration channel. As can be seen from Fig.7, the energy corresponding to the peak in the virtual RPA distribution increases of approximately 8 eV for each 4 eV increment of the reference electron temperature.

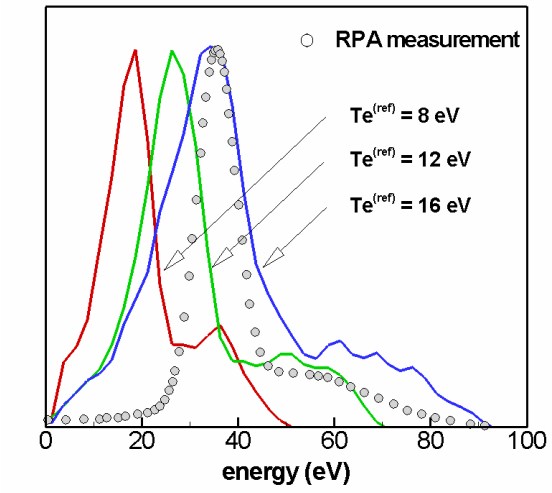

Fig.7 – Computed plasma energy distributions as a function of electron reference temperature.

At the same time, the secondary peak is smoothed out, and a high energy tail can be observed that is similar in

shape to the measured one. Correspondently, the width of the distribution increases.
The corresponding effect on current density distributions is illustrated in Fig.8. As a clear trend, the distribution becomes to some extent wider, starting approximately from 30°, as electron reference temperature is increased; correspondently, the maximum value recorded on the thruster axis diminishes.

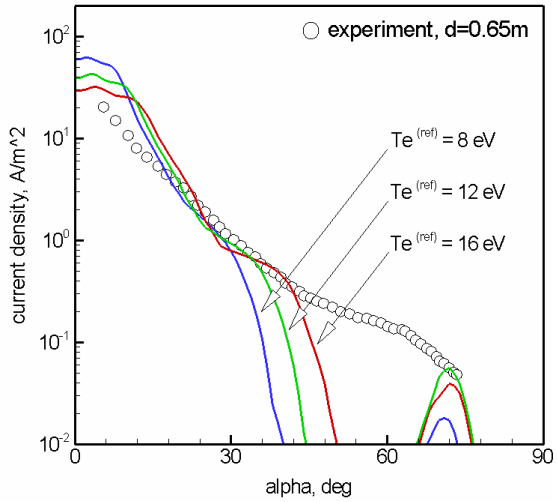

Fig.8 – Computed current density distributions as a function of electron reference temperature.

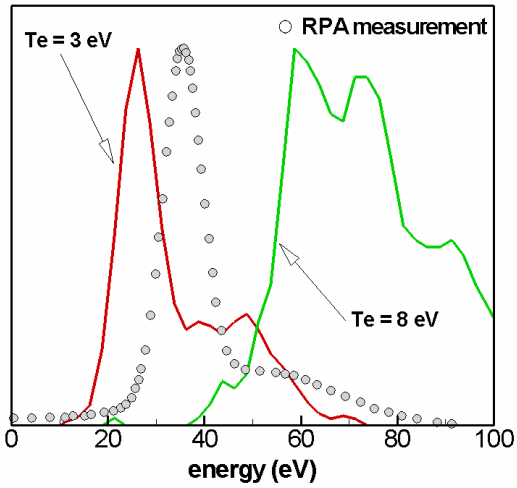

Fig.9 – Computed plasma energy distributions as a function of electron (constant) temperature.

Two simulations were subsequently carried out by using a constant value for electron temperature, set at 3 and 8 eV, respectively. In the first case, as shown in Fig.9, the energy distribution peak is found at approximately 26 eV; apart from this overestimation, the shape of the distribution appears in good agreement with the measured one. On the other hand, with electron temperature set to 8 eV CEX energies appear quite overestimated peaking at over 60 eV, and the width of the distribution becomes much wider with respect to experimental evidence. It is interesting to observe how, when electron temperature is retained constant, no energy contributions below approximately 15 eV are found.

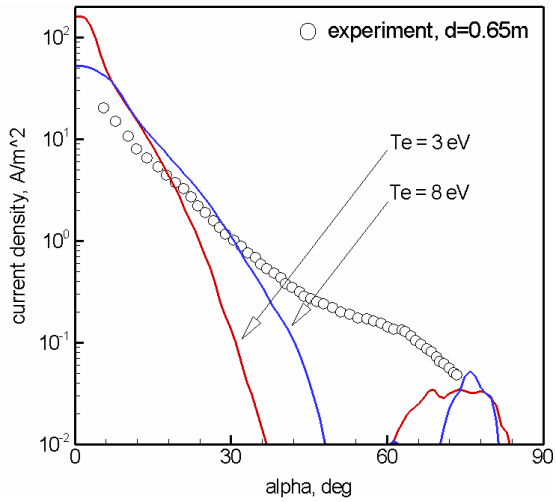

Fig.10 – Computed current density distributions as a function of electron (constant) temperature.

Fig.10 shows the computed current densities for constant electron temperature. The curves do not show the inflexion point which is observed at α=22÷28° with the adiabatic model; decreasing the electron temperature results in a sharper beam. Finally, Fig.11 shows the good agreement of the results obtained using a different collision model (VHS).

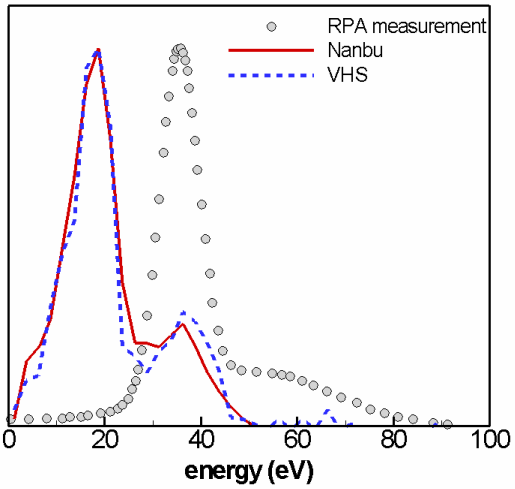

Fig.11 – Plasma energy distributions computed with different collision models.

For what concerns the electron temperature model effect it appears that, using the adiabatic model, realistic values for T_e and ion number density are obtained at the EPDP position compared to the flight data (see Table 2). It can be noted that the instrument seems to lay on the edge of the plasma plume and therefore be subject to relatively high variations of ion

number density (e.g. for case 1 between $3.7 \cdot 10^{13}$ and $7 \cdot 10^{13}$ m^{-3}); the possibility of EPDP location within the plasma sheath is consistent with the fact that the EPDP individuated a slightly non-neutral plasma. The plasma potential relative to the satellite surface is always predicted as slightly negative (between -2 V and -5 V) while the corresponding measurements present an almost constant value of +4 V. An increase in the T_e reference value corresponds to a shift of the RPA peaks towards higher values with and an increasing separation of the two peaks; a significant part of low energy events is recorded in any case.

Table 2 - Simulation results compared with EPDP data (continued)

Case	T_e model	T_e Ref [eV]	Collisions model	RPA Peak 1 [V]
1	Adiabatic	8	Nanbu	18.8
1b	Adiabatic	8	VHS	19.0
2	Adiabatic	12	Nanbu	27.1
3	Adiabatic	16	Nanbu	33.5
4	Constant	3	Nanbu	26.3
5	Constant	8	Nanbu	68.0
EPDP data				**35.6**

Table 2 - Simulation results compared with EPDP data (concluded)

RPA Peak 2 [V]	Peak distance [V]	FWHM [V]	EPDP rel. pot. [V]	EPDP Te [eV]	EPDP n_i x 10^{13} [m^{-3}]
36.1	17.3	12.9	-2.0	0.50	3.7 - 7
38.5	19.5	12.8	-2.2	0.56	3.6 – 7.2
49.2	22.1	13.5	-5.1	1.00	7 – 9
68.4	34.9	19.1	-5.5	1.10	5.4 – 6.8
43.8	17.5	11.6	-18.8	3.00	4.1
128.0	60.0	39.0	-50.0	8.00	3.2
55	**19.4**	**13**	**+4**	**0.62-0.72**	**6.8 – 8.7**

The use of a constant value for T_e produces RPA distributions which may resemble the measured one; on the other hand, the value of electron temperature giving the best agreement in a particular field point would probably be the wrong one when different positions are analyzed. Electron temperature value and relative potential are extremely different from the recorded ones, while ion number density is less than expected and close to the low limits for the adiabatic cases. An increase in the temperature value produces a significant shift of the peaks towards higher energies (as also noted by Boyd in [7]) and an overall *broadening* of the primary peak.

4. CONCLUSIONS

The essential features of the PICPlus3D code, a tool for the simulation of plasma thruster plumes, have been illustrated. The applications described focused on the simulation of the SNECMA PPS®1350 Hall thruster of the SMART-1 satellite, including comparison with experimental data from both vacuum chamber and flight conditions. An analysis of the influence of the electron temperature and collision models on the simulation results has been presented. Good agreement with flight data has been obtained by using ions exit conditions devised from fitting of vacuum chamber current density distributions, and finding appropriate values for electron temperature at the thruster exit. The physical models implemented in the simulation tool seem therefore adequate for a correct characterization of the features of the plasma plume; of course, use of the correct initial and boundary conditions is fundamental for the success of the simulation.

5. ACKNOWLEDGEMENTS

The authors wish to acknowledge the help provided by Mr. Jose Gonzalez del Amo and Mr. Eric Gengembre of ESA-ESTEC, Laben-PROEL for the SMART-1 in-flight data, and SNECMA Moteurs for the PPS®1350 ground test data.

6. REFERENCES

1. Boyd,I.D., *A Review of Hall Thruster Plume Modeling*, AIAA Paper 2000-0466, Jan. 2000.
2. Bird, G.A., Molecular Gas Dynamics and the Direct Simulation of Gas Flows, Oxford Science Publications, Oxford, 1994.
3. Andrenucci, M., Biagioni, L., Passaro, A., *PIC/DSMC Models for Hall Effect Thruster Plumes: Present Status and Ways Forward*, AIAA Paper 2002-4254, July 2002.
4. Nanbu, K., *Probability Theory of Electron-Molecule, Ion-Molecule, Molecule-Molecule, and Coulomb Collisions for Particle Modeling of Materials Processing Plasmas and Gases*, IEEE Transactions on Plasma Science, Vol.28, No.3, 2000.
5. Matticari, G., Noci, G., Estublier, D., Gonzales del Amo, J., Marini, A., Tajmar, M., *The Smart-1 Electric Propulsion Diagnostic Package*, proceedings of the 3rd Spacecraft Propulsion Conference, 2000.
6. Biagioni, L., Passaro, A., *Vicini*, A., *Plasma Thruster Plume Simulation: Effect of the Plasma Quasi Neutrality Hypothesis,* 34th AIAA Plasmadynamics and Lasers Conference, Orlando FL , 23-26 June 2003.
7. Boyd, I. D., "Hall Thruster Far Field Plume Modeling and Comparison with EXPRESS Flight Data", AIAA Paper 2002-0487, 2002.